LM-04K054
June 10, 2004

New Performance Levels for TPV Front Surface Filters

TD Rahmlow, JE Lazo-Wasem, EJ Gratrix, PM Fourspring, and DM DePoy

New Performance Levels for TPV Front Surface Filters

Thomas D. Rahmlow, Jr, Jeanne E. Lazo-Wasem and Edward J. Gratrix

Rugate Technologies, Inc, Oxford, CT 06478

Patrick M. Fourspring and David M. DePoy

Lockheed Martin Company, Schenectady, NY 12301

Abstract. Front surface spectral control filters significantly improve the efficiency of thermophotovoltaic (TPV) converters. Tandem filter designs for 0.52 and 0.60 eV cells were fabricated. Energy and angle weighted spectral efficiencies of ~83% for the 0.52 eV application and ~76% for the 0.60 eV applications were achieved with ~78% angle weighted above bandgap transmission. Manufacturing demonstrations of both designs were completed with good yield. Design improvements were made using angle weighted spectral utilization and above bandgap transmission as refinement goals. Current development work addresses elimination of the plasma filter and alternate substrates.

INTRODUCTION

Thermophotovoltaics (TPV) provide direct conversion of radiant thermal energy to electricity. The key components of a high efficiency TPV system includes a radiative heat source, a TPV cell on the cold side, a cold side radiator or heat sink, thermal insulation and a means of spectral control. The TPV cell, like a solar cell, converts absorbed above bandgap photons to electric energy. The advantage of TPV direct energy conversion over solar cells is the potential for high flux densities and high conversion efficiencies with no moving parts. Spectral control is critical to achieving high TPV system efficiency. The spectral control scheme must allow the passage of above bandgap photons to the TPV cell for conversion and suppress or return below bandgap photons to the heat source for recuperation. Figure 1a presents a sketch of a TPV system using front surface filters as the spectral control scheme. Figure 1b plots incident flux for parallel flat plate geometry. Peak incident flux at the filter is at an angle of incidence (AOI) of 45^o.

Front surface filters are placed between the heat source and the TPV cell. The front surface filter allows above bandgap photons to pass through the filter into the TPV cell while reflecting below bandgap photons back towards the heat source. Thermal contact between the front surface filter and the TPV cell allows the filters to be kept cool. Figure 2a presents measured reflection for a front surface filter at 45^o AOI and the emission spectra for a black body source at 950 ^{o}C. The front surface filter is a broadly reflecting non-polarizing short pass edge filter. The transition edge from highly transmitting to highly reflecting is sharp and placed at the wavelength of the TPV cell's bandgap.

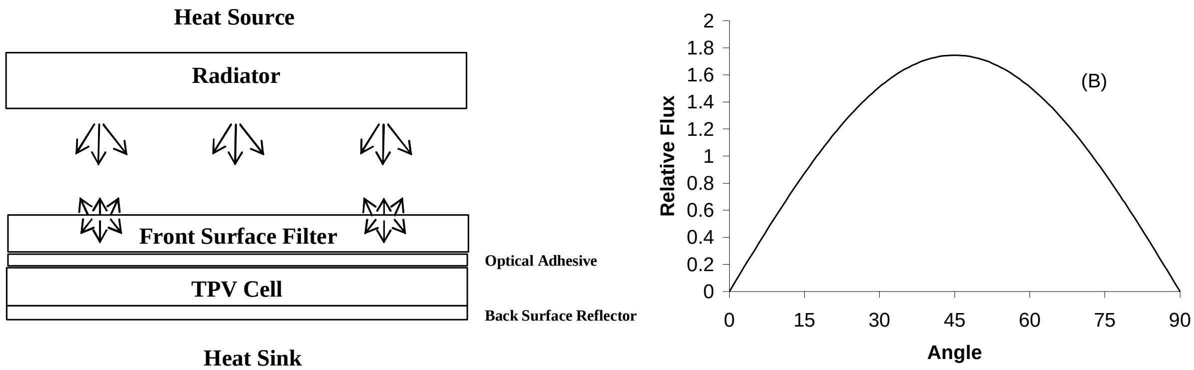

Figure 1: Front surface filters are placed on the cold side of a TPV converter in front of the TPV cell. The filter allows above band gap photons to pass through into the TPV cell and reflects long wavelength photons back to the source. Incident flux (B) for flat plate geometry is peaked at 45^o.

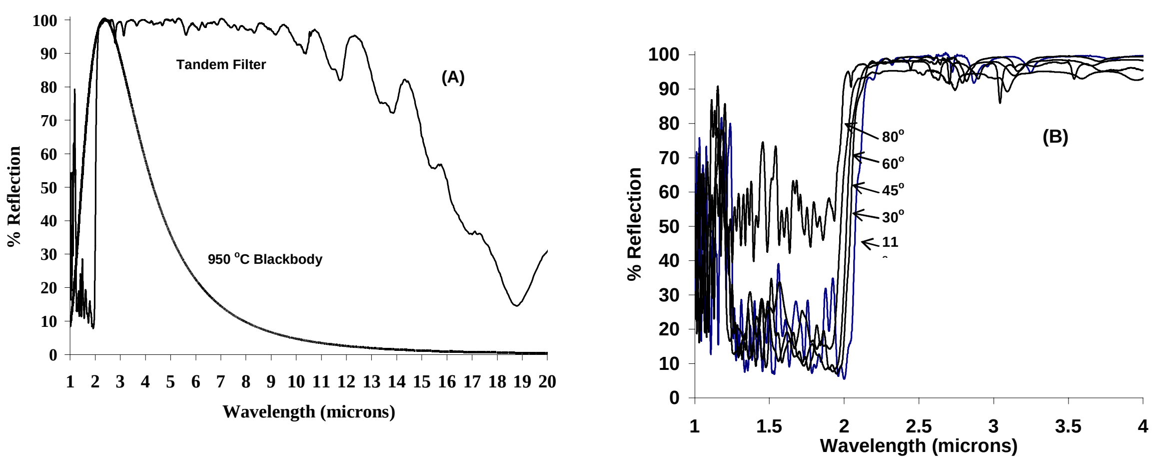

Figure 2: Measured reflection of a front surface tandem filter (A) is plotted along with a black body spectrum for 950 ^{o}C. The filter's transition edge is placed at the cell's band gap. High reflection of below band gap photons is needed to achieve high spectral efficiency. Measured reflection measurements of a 0.6 eV front surface filter (B) highlight the shift of the transition edge with angle of incidence (AOI). The pass band transmission degrades at near grazing angles.

The front surface filter must perform well over all incident angles from near normal to near grazing. The peak in radiator flux is at 45^o AOI and is continuously distributed over all angles. This is a concern for interference filter designs since interference filter performance shifts towards shorter wavelengths with increased angles of incidence. Figure 2b presents transmission measurements of the filter's transition edge from 11^o to 80^o AOI. The edge position at 45^o AOI is just short of the TPV cell's bandgap. Spectral efficiency of this filter is calculated from spectral measurements to be 77.3 % with a black body source at 950 ^{o}C.

Spectral efficiency is the ratio of absorbed above bandgap energy reaching the TPV cell to the total energy absorbed [1]. Spectral efficiency is a function of both the radiator spectrum and the angle weighted distribution of the flux. The same front surface filter will have a different spectral efficiency for different incident spectra. The spectral efficiency of these designs is calculated from modeled transmission and reflection spectra over the wavelength range of 0.5 to 25 microns at a range of angles from 5 to 85^{o} in increments of 5^{o} and a black body source at 950 ^{o}C. The spectral efficiency for fabricated filters is calculated from spectral measurements at 11, 30, 45, 60 and 80^{o} AOI and the calculated performance of a black body source.

DESIGN DEVELOPMENT AND REFINEMENT

The front surface filter design is a tandem filter [2, 3] consisting of an interference short pass filter on a plasma filter substrate. The interference filter defines the transition edge at the TPV's bandgap and provides high below bandgap reflection out to beyond 6.5 microns. The plasma filter is a 1 micron InPAs layer doped nominally to 5E19 on an InP substrate. The plasma layer provides high reflection at about 6 microns and longer. Below 3 microns, the plasma filter is transmissive. Figure 3a presents the measured spectrum of a tandem filter, the plasma filter alone and the interference filter on a silicon substrate. Figure 3b presents absorption calculated from measured transmission and reflection for the tandem filter. The heavily doped plasma layer contributes about 3.5% integrated absorption in the above bandgap region. The interference filter materials are strongly absorbing at long wavelengths.

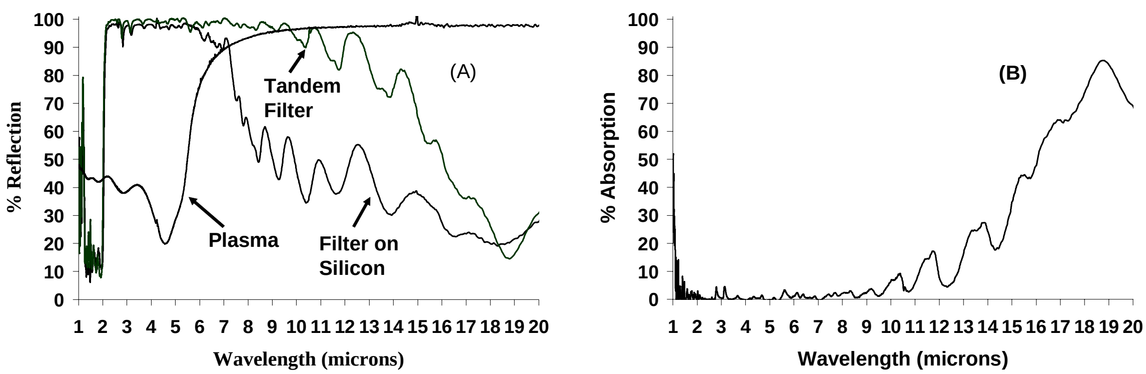

Figure 3: The tandem filter is a multilayer interference filter on a plasma filter. Measured reflection of the tandem filter, the plasma filter and interference filter a silicon substrate are overlaid (A). Measured absorption of the tandem filter is also plotted (B).

Figures 4a through 4d present the impact of increasing the complexity of the 0.52 eV front surface filter design and the inclusion of a plasma layer. The first design, figure 4a, is a simple quarter (QW) wave stack interference filter without a plasma layer. It offers a spectral efficiency of about 43%. Figure 4b presents a multi-stack interference filter with a plasma layer. Modeled spectral efficiency is 81% with the plasma layer contributing about 15% of this efficiency. Current tandem designs, figure 4c, offer greater than 85% spectral efficiency, with the plasma layer contributing about 3%. Figure 4d presents a design without a plasma layer with performance comparable to a tandem filter. The reflection of the interference filter at long wavelengths is not quite as good as the tandem filter design, but above bandgap absorption due to the plasma layer is eliminated. Table 1 shows the spectral efficiency and above band gap transmission for each design refined with and without a plasma layer.

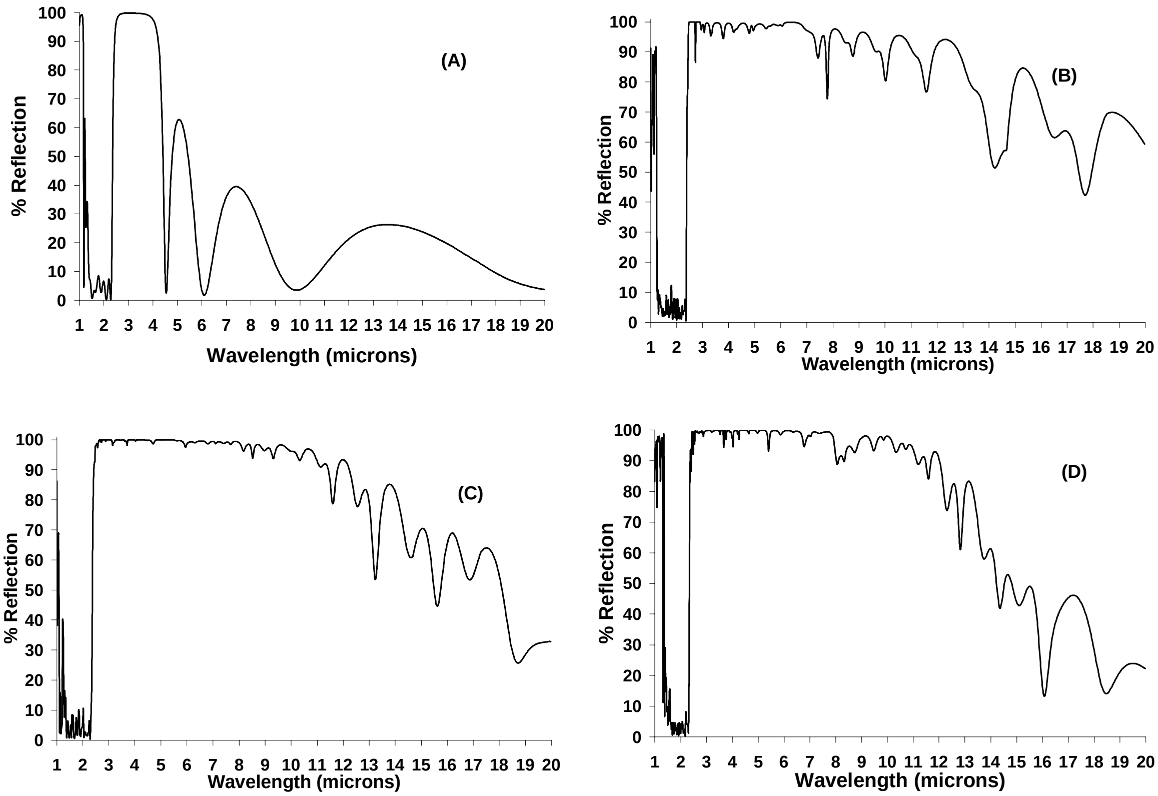

Figure 4: (A) Predicted reflection for a single QW notch filter design (without plasma) – spectral efficiency is 43%. (B) Predicted reflection for a target refined tandem filter design (with plasma) – spectral efficiency is 81%. (C) Predicted reflection for a Goal Driven Refined (GDR) tandem filter design (with plasma) – spectral efficiency is 85%. (D) Predicted reflection for a Goal Driven Refined (GDR) tandem filter design with additional layers (without plasma) – spectral efficiency is 85%

Table 1: Comparison of Design Performance (0.52 eV)

Design	With Plasma		Without Plasma	
	Spectral Eff	>Eg Tr	Spectral Eff	>Eg Tr
QW	-	-	43	66
Target Refined	81	80	67	83
GDR	85	<82	83	>82
GDR with additional layers	85	74	85	77

Initial design development was done with Optilayer™. This is a commercially available filter design code that incorporates needle synthesis as well as traditional refinement methods. Needle synthesis is a software design technique by which a thin layer (needle) of material is moved through a design and inserted at the point where a merit function is most improved. The thickness of the layer is then refined further using a conventional refinement algorithm such as gradient descent. The targets used are the desired transmission and reflection spectrum. Typically, a reasonable starting design is needed to produce a solution that can be manufactured. Our experience is that very good solutions were obtained using needle synthesis for designs with very large numbers of films (greater that 150 layers). Designs with a practical limit of 50 to 90 layers obtained spectral efficiencies of 65 to 74 % for 0.6 eV filters and 77 to 81% for 0.52 eV filters.

An alternative design refinement technique that has proven effective is Goal Driven Refinement (GDR). GDR uses a merit function derived from the desired performance goals. In this case, spectral efficiency and above bandgap transmission are the refinement goals rather than transmission and reflection targets. Spectral utilization incorporates the impact of incident angle and energy distribution into a single number. Traditional refinement targets define a desired reflection and transmission spectrum. Multiple targets at different angles can be defined, offset for angle shift and individually weighted, but the process requires that the targets be self consistent. GDR takes the impact of angle shift and radiator spectrum directly into account. The merit function used is the square root of the sum of the difference between the goal and the calculated values for the spectral efficiency and above band gap transmission.

A consequence of using the GDR technique is that each design can be systematically refined using a matrix of relative values for the design goals (spectral efficiency versus transmission). By changing the value of the individual goals, the merit function is weighted in favor of one goal versus the other. The result is a family of related designs. Each design has the same number of layers and very similar layer thickness.

Figures 5a and 5b plot refinement results for a series of designs developed for 0.6 eV and 0.52 eV respectively. The refinement matrix for different designs is plotted as a function of transmission versus spectral efficiency. The result is a single curve illustrating the trade-off between spectral efficiency and transmission. When the design that was optimized using traditional target refinement techniques was further refined using GDR, a significant improvement in spectral efficiency was obtained. The impact of adding additional layers and the point of diminishing return is also well illustrated in these figures.

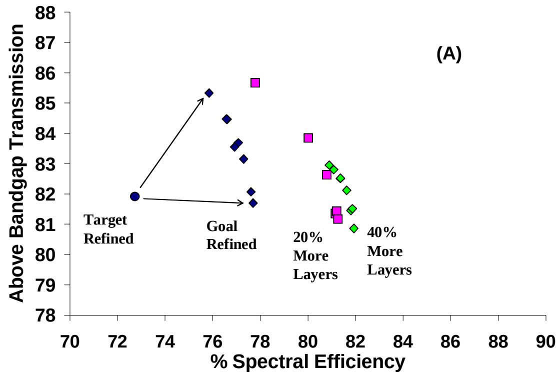

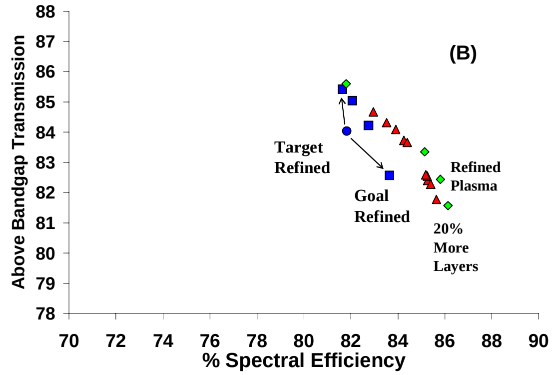

Figure 5: Design Evolution for 0.6 eV designs (A) and 0.52 eV designs (B). The trade-off between spectral Efficiency and % Above Bandgap transmission is plotted. Strong gains in spectral efficiency are achieved by goal refinement of the single transmission and reflection target refined design.

Characterizing Design Performance

The performance of front surface tandem filters is determined by the physical behavior of the interference and plasma filter. The spectral performance of the interference filter shifts towards shorter wavelength with increased angle of incidence. Filter performance will also degrade as a result of polarization effects. The plasma filter does not significantly change with incidence angle. The result is that a region of reduced reflection can open up between the interference filter and the plasma filter. To avoid this, the interference filter is designed to significantly over lap the plasma filter at normal AOI.

Spectral efficiency, above band gap transmission and below bandgap reflection are plotted as a function of angle in figure 6a. Spectral efficiency is relatively flat for angles up to about 60^{o} and then falls off. Above bandgap transmission begins to fall off after 45^{o} as the edge moves into the passband. Two effects limit transmission at high AOI. The first is that the transition edge is moving shorter with higher angles and is now in the filter transmission band. The second effect is the increase in reflection as the angle of incidence approaches the grazing angle. In general, GDR refines the design for best performance which may not necessarily be at 45^{o} AOI. This is due to the asymmetry in filter performance with angle.

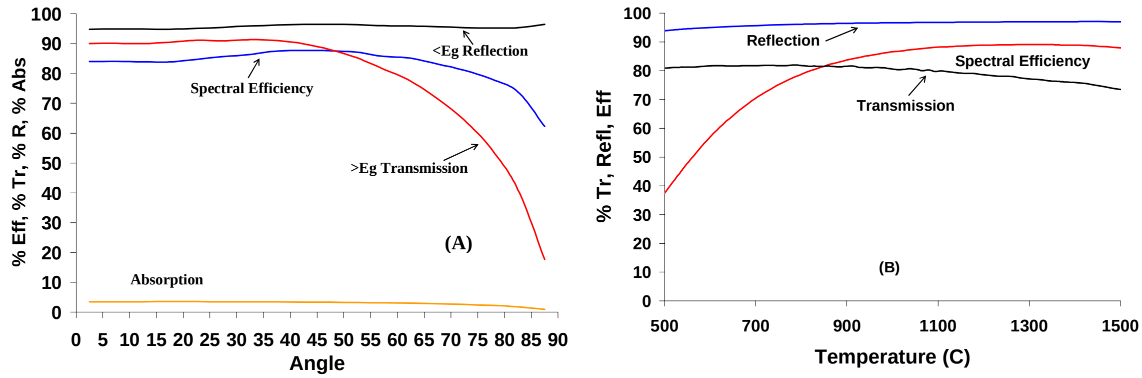

Figure 6: Spectral efficiency, above bandgap transmission and below band gap reflection is plotted as a function of incident angle (A). Spectral efficiency and above band gap transmission as a function of radiator temperature is plotted for a 0.52 eV filter (B).

The spectral efficiency of a filter design is a function of the radiator spectrum and therefore the radiator's temperature. Figure 6b presents spectral efficiency and above bandgap transmission for the filter as a function of the black body radiator temperature but constant bandgap. Efficiency improves as the radiator temperature increases and more above bandgap photons are available.

FILTER FABRICATION RESULTS

Several tandem filter designs have been fabricated with good results. TPV cells with a 0.6 eV band gap and a tandem filter achieved efficiencies in excess of 20% with in-cavity efficiency tests [4]. Figures 7a and 7b present an overlay of expected and measured reflection for 0.6 eV and 0.52 eV filters at 45 AOI. The results show good agreement between measured and fabricated performance. Manufacturing demonstrations in which multiple filters per run and multiple runs in series, with no changes to the filter design or chamber calibration, have been completed for both 0.6 eV and 0.52 eV applications. For 0.6 eV, three 3" filters per run were coated and three runs were executed in series. For 0.52 eV, four 2" filters per run and 12 runs were executed in series.

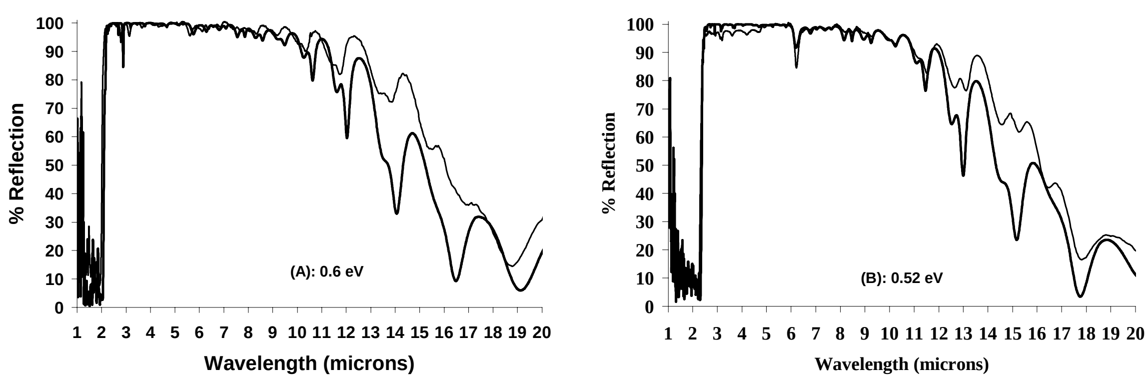

Figure 7: Expected and measured reflection at 45^{o} AOI is overlaid for the (A) 0.6 eV and (B) 0.52 eV designs.

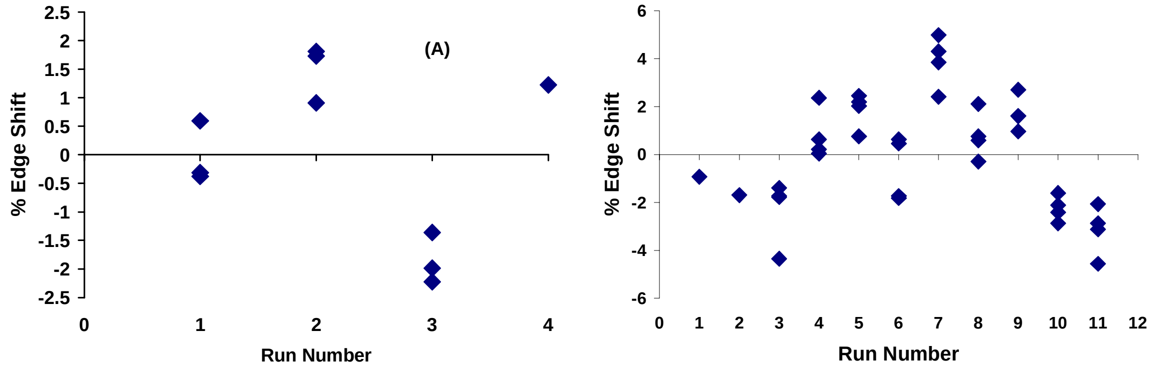

Figure 8: Percent Edge shift with-in run and from run to run are plotted for the 0.6 eV manufacturing demonstration (A) and for the 0.52 eV manufacturing demonstration (B).

Run to run stability is presented in figures 8a and 8b. These figures plot the variation in the location of the transition edge for filters coated in the same run and filters coated from run to run. Variance in edge position within the same run is 0.5 to 1%. Variation from run to run was about 1.5 to 6%. Figures 9a and 9b present overlays of the transmission edge at normal AOI for all filters fabricated in these two manufacturing demonstrations.

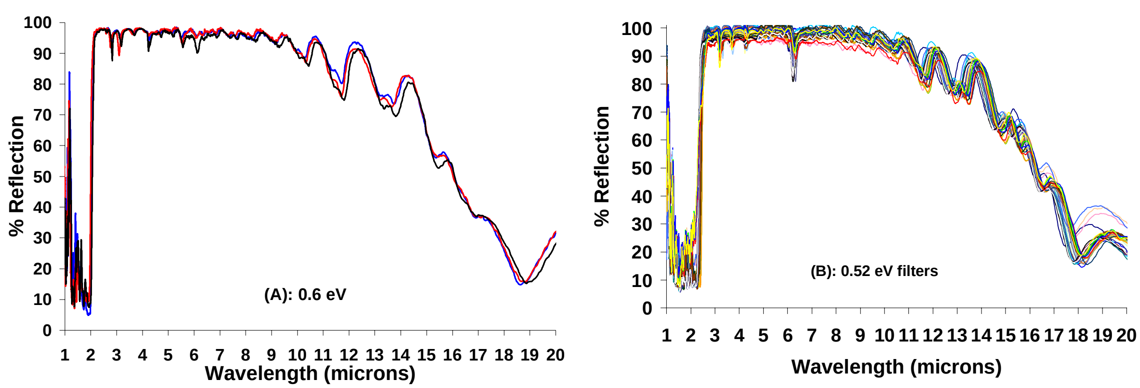

Figure 9: Reflection measured for 0.6 eV filters samples from three runs are overlaid (A). Measurements are at 45^{o} AOI. Measured reflection for all 36 0.52 eV filters are overlaid (B).

CONCLUSIONS

Front surface filters are a practical means of providing high efficiency spectral control in TPV systems. The successful completion of two manufacturing demonstrations of 0.52 eV and 0.6 eV filters demonstrate that the filters can be reliably fabricated with high yield and good performance. For 0.52 eV filters, a spectral efficiency of 83% has been achieved with an angle weighted above bandgap transmission of 79%. For the 0.6 eV filters, a spectral efficiency 76% has been achieved with an angle weighted above bandgap transmission of 78%. Front surface filters with 0.6 eV TPV cells have achieved a measured, in-cavity efficiency of greater than 20% [4].

Improvements to the filter design codes using spectral utilization and above band gap transmission merit functions facilitate the development of new designs, designs for alternate band gaps and designs optimized for alternate radiator characteristics.

The design of front surface filters is evolving. The quality of the interference filter is much improved over older designs. The interference filter reflection of current designs extends out beyond 9 microns. The role of the plasma layer in the tandem design is becoming less important as new high efficiency designs using the interference filter alone are being developed. Deposition on non-semiconductor substrates and on altered plasma filter substrates is possible. While filter fabrication is still at the prototype level, deposition yields are improving making direct deposition on TPV cells and elimination of a separate substrate and glue is becoming plausible.

REFERENCES

1. Baldasaro, P.F., et al., *Thermodynamic Analysis of Thermophotovoltaic Efficiency and Power Density Tradeoffs.* Journal of Applied Physics, 2001. **89**: p. 3319-3327.
2. DePoy, D.M., et al., *Interference Filters for Thermophotovoltaic Applications*, in *Optical Interference Coatings*. 1998, Optical Society of America. p. ThC5-1, ThC5-2.
3. Hickey, C.F., M. Trahan-Verma, and D.M. DePoy, *Antimony Selenide in Multilayer Coatings*, in *Optical Interference Coatings*, T.J. Coutts, J.B. Benner, and C.S. Allman, Editors. 2001, Optical Society of America. p. ThE4-1, ThE4-3.
4. Wernsman, B., et al., *Greater than 20% Radiant Heat Conversion Efficiency of a Thermophotovoltaic Radiator / Module System Using Reflective Spectral Control.* IEEE Transactions on Electron Devices, 2004. **51**(3): p. 512-515.